Selective Electron- or Hole-Transport Enhancement in Bulk-Heterojunction Organic Solar Cells with N- or B-Doped Carbon Nanotubes

Ju Min Lee, Ji Sun Park, Sun Hwa Lee, Hoyeon Kim, Seunghyup Yoo, and Sang Ouk Kim**

Most current high-efficiency organic solar cells consist of a bulk heterojunction (BHJ) of semiconducting polymers and fullerene derivatives.[1,2] The enormous donor–acceptor interfacial area of the BHJ maximizes the opportunity for exciton dissociation, overcoming the short exciton diffusion lengths of organic materials.[3] The BHJ structure, however, is often considered less optimal for charge transport due to the lack of dedicated pathways for each type of carrier.[4] This morphological limitation of the BHJ, along with the intrinsic slow transport properties of organic semiconductors, makes it challenging to utilize the full potential of organic solar cells.[5]

One straightforward way to address the retarded carrier transport in organic solar cells is to incorporate one-dimensional nanomaterials, such as nanorods[6–8] or nanotubes,[9–13] within semiconducting materials. In this regard, carbon nanotubes (CNTs) are an ideal material, as they have excellent carrier mobility, mechanical flexibility, and compatibility with the solution process.[14–16] Despite these conceptual advantages, however, solar cells with CNTs incorporated in their semiconducting active layers have demonstrated significantly poorer performance than those without CNTs.[10,17] Without charge selectivity, any small proportion of metallic CNTs present may build up undesired pathways for electron–hole recombination.[9] Furthermore, inhomogeneously dispersed CNT aggregates give rise to a fatal device short circuit.

Here we present the remarkable device performance enhancement in BHJ solar cells employing N- or B-doped CNTs (N-CNT or B-CNT) as highly selective electron- or hole-transport enhancement materials. We used commercially available multiwalled CNTs. Due to their multiwalled nature, the undoped CNTs are metallic. The B-doping of CNTs was performed by using thermal treatment with vaporized B_2O_3 under an Ar/NH_3 gas flow mixture.[18] The NH_3 was introduced as an etching gas to induce vacancy defects with CN_x and C_xH_y groups. Further reaction with vaporized boron resulted in the substitutional B-doping of CNTs.[19] **Figure 1**a is the electron energy loss spectroscopy (EELS) K-edge spectrum of the resultant B-CNT.[18–21] The π^*-peak of the boron K-edge observed at 190 eV indicates that boron atoms are sp^2 -hybridized, like their carbon counterparts. The nitrogen K-edge peak observed at 400 eV indicates that a small amount of nitrogen atoms are doped into the CNTs. For N-doping, a similar thermal treatment was performed but without B_2O_3. Figure 1b shows the EELS spectrum of the N-CNT. The π^*-peak of the nitrogen K-edge indicates that nitrogen atoms are doped into the CNT, maintaining the sp^2-hybridized structure of the CNTs. Quantitative doping-level measurements by X-ray photoelectron spectroscopy (XPS), elemental analysis (EA), and inductively coupled plasma–mass spectroscopy (ICP-MS) demonstrate that B-CNTs were 3.0 atom% B-doped and 0.5 atom% N-doped, while N-CNT was 3.4 atom% N-doped. (See Supporting Information Figure S1).[22,23]

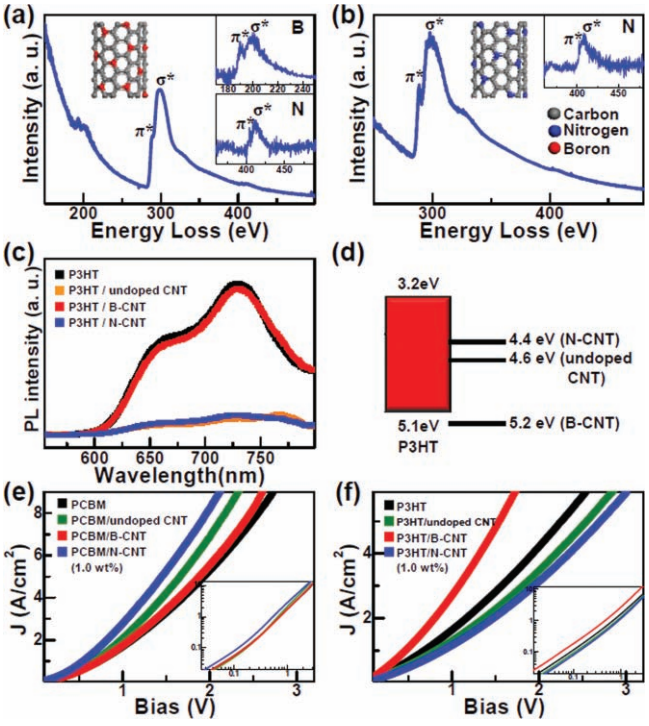

Figure 1. EELS K-edge spectra of a) B-CNT and b) N-CNT. c) Photoluminescence spectra and d) schematic energy diagram of P3HT/CNT films. *J–V* characteristics of e) electron-only and f) hole-only devices. The slope of *J–V* curve in logarithmic scales was two [insets of (e) and (f)].

J. M. Lee, J. S. Park, S. H. Lee, Prof. S. O. Kim
Department of Materials Science and Engineering
KI for the Nanocentury, KAIST
Daejeon, 305–701, Republic of Korea
E-mail: sangouk.kim@kaist.ac.kr
H. Kim, Prof. S. Yoo
Department of Electrical Engineering
KAIST, Daejeon, 305–701, Republic of Korea
E-mail: syoo@ee.kaist.ac.kr

DOI: 10.1002/adma.201003296

We investigated the interaction of the doped CNT with the photoexcited electrons in a semiconducting polymer, poly 3-hexylthiophene (P3HT), by photoluminescence (PL) spectroscopy (Figure 1c). 60-nm-thick P3HT/CNT blend films were prepared by solution casting. The photoexcited electrons generated within P3HT transferred to the undoped CNTs or N-CNTs, and, thus, the PL emission was quenched. However, the photoexcited electrons do not interact with B-CNTs, such that the original PL spectrum of the pure P3HT polymer was regenerated. For an efficient electron or hole transport at the organic semiconductor–metallic multiwalled CNT interface, the CNTs should have a work function that closely matches with the lowest unoccupied molecular orbital (LUMO) or the highest occupied molecular orbital (HOMO) of the neighboring semiconducting materials.[24–26] The work function of the undoped CNT measured by ultraviolet photoemission spectroscopy (UPS) was 4.6 eV (Supporting Information Figure S2).[27] Since boron has one less electron than carbon, the B-doping decreases the π electrons and thus increases the work function of the B-CNT up to 5.2 eV. In contrast, the work function of the N-CNT decreased down to 4.4 eV, due to the additional π electrons from the doped nitrogen atoms. As shown in Figure 1d, the work function of the N-CNT matches well with the LUMO of the [6,6]-phenyl-C_{61}-butyric acid methyl ester (PCBM), while that of the B-CNT matches well with the HOMO of P3HT. This variation of work function clearly explains the selective transfer of photoexcited electrons, presented in Figure 1c.

While the transport properties of organic semiconductors are intrinsically retarded by intermolecular or interchain hopping process, incorporation of charge- selective, doped CNT is anticipated to enhance the carrier transport. For example, an N-CNT may play the role of a "bridge", helping electron transfer between PCBM molecules. Likewise, incorporation of B-CNT into P3HT can enhance the hole transport in P3HT films. The effect of doped CNTs on the transport properties of P3HT or PCBM films was demonstrated by the DC current density (*J*)–voltage (*V*) characteristics of the electron-only (Figure 1e) and hole-only (Figure 1f) devices.[28] The PCBM-based electron-only device consists of indium-doped tin oxide (ITO), Cs_2CO_3, PCBM/CNT, and Al layers. The ITO and Cs_2CO_3 bilayer blocks the hole injection to PCBM (Supporting Information Figure S3a).[29] As shown in Figure 1e, the device with 1.0 wt% N-CNT shows an improved electron transport over the undoped device. Since the work function of N-CNT (4.4 eV) is close to the LUMO of PCBM (4.2 eV), the N-CNT can readily accept electrons from PCBM, which effectively transport through the long lengths of the CNTs (<1 μm) and transfer to a neighboring PCBM molecule. The undoped CNT also demonstrates a weak transport enhancement. However, incorporation of the B-CNT fails to enhance the transport properties of PCBM due to the large work function of B-CNT (5.2 eV). The P3HT-based hole-only device consists of ITO, poly(3,4-ethylenedioxythiophene) poly(styrenesulfonate) (PEDOT:PSS), P3HT/CNT, WO_3, and Al layers, where the Al and WO_3 bilayer prevents electron injection (Supporting Information Figure S3b).[30] As shown in Figure 1f, the device with 1.0 wt% B-CNT showed a remarkable enhancement in *J*, while those with 1.0 wt% N-CNT or undoped CNT showed a decrease in *J*. This result is again consistent with the fact that the work function of B-CNT matches well with the HOMO of P3HT. Meanwhile, the carrier-mobility calculation based on Mott–Gurney law,[31,32] revealed that the electron-only and hole-only devices with 1.0 wt% B-CNT had quite well-matching electron and hole mobilities of 1.3×10^{-7} m^2 V^{-1} s^{-1} and 1.6×10^{-7} m^2 V^{-1} s^{-1}, respectively; such matching is greatly desired for high-performance optoelectronic devices (Supporting Information **Table 1**).[33]

Table 1. Solar cell device characteristics including power conversion efficiency (PCE), open circuit voltage (V_{oc}), short circuit current (J_{sc}), and fill factor (FF).

	PCE [%]	V_{oc} [V]	J_{sc} [mA cm^{-2}]	FF [%]
without CNT	3.0	0.54	9.08	61.5
undoped CNT 0.2%	3.2	0.58	8.52	65.3
undoped CNT 1.0%	2.6	0.52	7.69	64.4
undoped CNT 3.0%	1.3	0.47	6.69	42.7
undoped CNT 5.0%	1.1	0.45	6.06	41.0
B-CNT 0.2%	3.3	0.55	9.79	61.8
B-CNT 1.0%	4.1	0.57	11.47	61.3
B-CNT 3.0%	2.6	0.53	8.34	59.0
B-CNT 5.0%	2.3	0.54	6.77	61.8
N-CNT 0.2%	2.8	0.52	9.10	58.0
N-CNT 1.0%	3.7	0.55	10.41	63.8
N-CNT 3.0%	1.2	0.43	7.80	35.0
N-CNT 5.0%	0.2	0.11	7.60	26.1
B- & N-CNT 0.2%	3.0	0.56	9.29	57.5
B- & N-CNT 1.0%	2.1	0.53	9.19	43.9
B- & N-CNT 3.0%	0.9	0.33	8.65	31.0
B- & N-CNT 5.0%	0.7	0.30	8.17	27.9

The observed mobility enhancement with doped CNTs effectively improves the efficiency of BHJ organic solar cells. The P3HT/PCBM/CNT BHJ solar cell fabricated in this work is described in **Figure 2**a. The 30-nm-thick TiO_x layer played the role of optical spacer.[34,35] Figure 2c shows the *J*–*V* characteristic of solar cells with 1.0 wt% CNTs, or without CNT. The *J*–*V* characteristic of the solar cells without CNT give an open circuit voltage of 0.54 V, a short-circuit current density of 9.08 mA cm^{-2}, and a fill factor of 61.5%, which lead to an overall power conversion efficiency of 3.0%. The solar cells with 1.0 wt% undoped CNT exhibited a poorer performance, with a J_{sc} value of 7.69 mA cm^{-2}, which indicates that the undoped CNTs became undesired pathways for electron–hole recombination.[9] In contrast, solar cells with N-CNTs or B-CNTs showed an enhancement in J_{sc} and PCE. In particular, those with B-CNTs exhibited the largest enhancement of J_{sc} and PCE, up to 11.74 mA cm^{-2} and 4.1%, respectively. This result is consistent with the observation that the B-CNT may balance electron and hole transport. Incorporation of B-CNT and N-CNT mixtures, however, resulted in significantly worse performance than for the undoped device, which is attributed to the bundling of electron-accepting and hole-accepting CNTs, as discussed below. Figure 2d compares the *J*–*V* characteristics of organic solar cells with 1.0 and 3.0 wt% B-CNT. The J_{sc} and PCE have the highest values for 1.0 wt% of B-CNT. The same trend was observed for

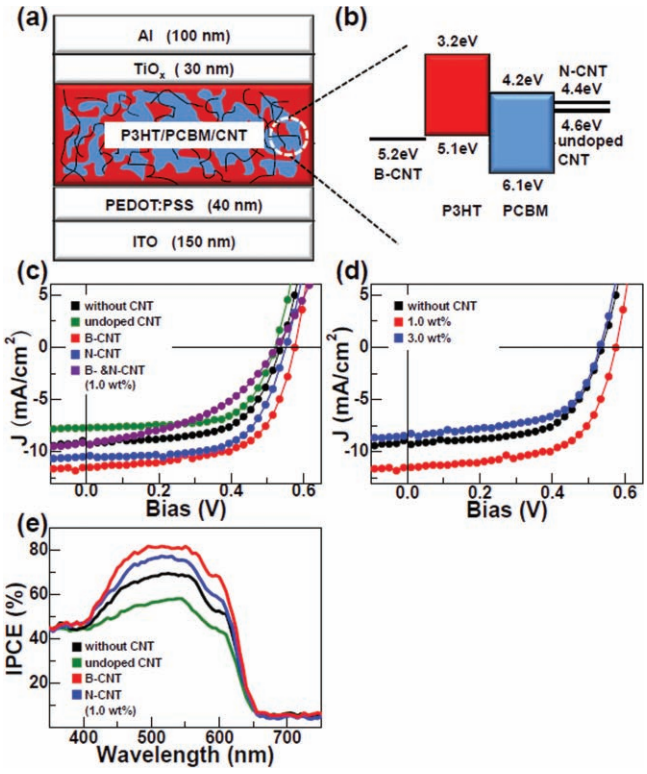

Figure 2. a) Schematic device structure and b) energy diagram of a solar cell with CNTs. c) *J–V* characteristics of the different solar cells. d) *J–V* characteristics of the solar cells e) IPCE spectra of the solar cells with or without CNTs.

solar cells with N-CNT. Table 1 summarizes the detailed device characteristics, including PCE, V_{oc}, J_{sc}, and FF for all solar cells fabricated in this work.

Figure 2e shows the incident photon to current conversion efficiency (IPCE) spectra of the organic solar cells. The device with B-CNTs shows the highest IPCE values over the entire wavelength range, followed by the solar cell with N-CNT or without CNT. The maximum IPCE values for the devices with B-CNT and N-CNT, measured at 550 nm, were 82% and 77%, respectively. The overall integral of the IPCE and the AM1.5G (1 Sun) reference spectra yields a J_{sc} value of 9.0 mA cm^{-2} for the solar cell without CNT, 11.1 mA cm^{-2} with B-CNT, 10.0 mA cm^{-2} with N-CNT, and 7.43 mA cm^{-2} with undoped CNT, which agree well with the J_{sc} values measured above. Together with the *J–V* results obtained under AM1.5G illumination, the IPCE measurements show that the short-circuit current density, and thus the device efficiency, of the organic solar cells are remarkably enhanced with B- or N-CNT.

We have confirmed that doped CNTs in the BHJ active layer are highly desirable for solar cell performance. Along with their selective carrier-transport enhancement, fine dispersibility in the active layer is also crucial to avoid aggregation-induced performance degradation. The dispersibility of undoped and doped CNTs was evaluated by optical microscope observation (**Figure 3**a).[36–39] 80–90-nm thick active layer films were spin cast and thermally treated (15 min at 150 °C). In the active layer with undoped CNTs, strong van der Waals interaction causes the bundling of the CNTs. As shown in Figure 3a, many dark aggregates appear even at 1.0 wt%. In contrast, B- or N-doping remarkably improves the dispersibility of the CNTs. The density of dark aggregates was significantly lowered, even at 3.0 wt%. In the case of boron, the doped sites yield local positive charges which induce an electrostatic repulsion with neighboring B-CNTs. Moreover, the local polarity induced by boron–carbon bonding may enhance the dispersibility in organic solvents and the polymer matrix. The nitrogen atoms in N-CNTs may cause

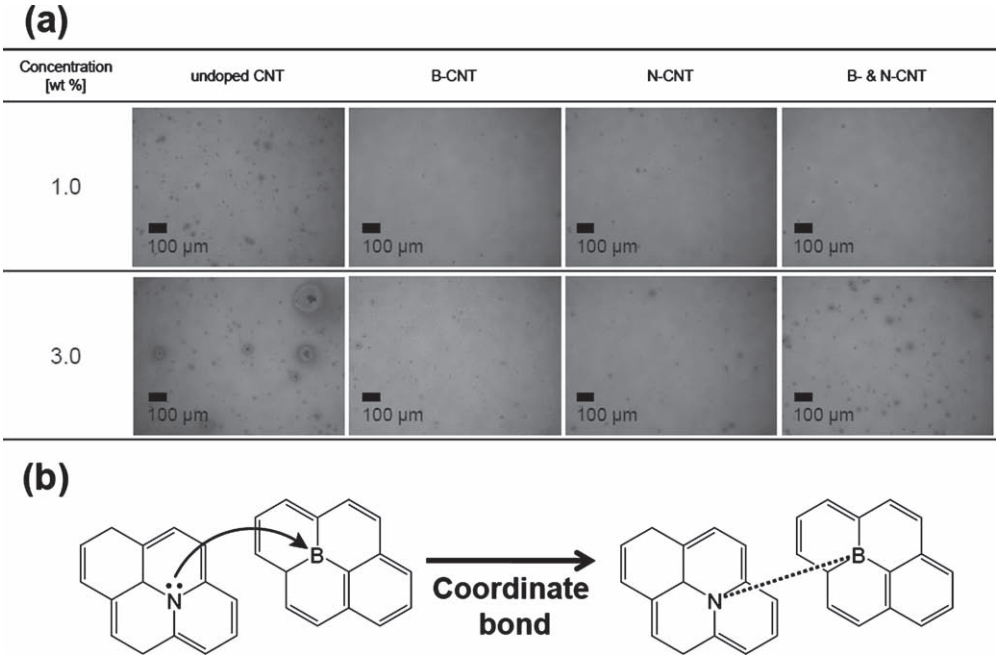

Figure 3. a) Optical microscopy images of P3HT/PCBM BHJ active layers with or without CNTs. b) Coordination interaction between B- and N-CNTs. The boron atoms in B-CNTs attract the lone-pair electron of the nitrogen atom in N-CNTs.

local negative charges and local polarities. In the case of the B- and N-CNT mixture, the boron atoms in B-CNT may attract the lone-pair electron of the nitrogen atom in N-CNT to form coordinate bonding (Figure 3b). This relatively strong interaction causes the aggregation of CNTs, as observed in Figure 3a. This hypothesis is consistent with the lower device performance of organic solar cells with a mixture of B-CNT and N-CNT.

In summary, we have demonstrated the highly selective carrier-transport enhancement and the corresponding power-conversion-efficiency improvement of P3HT/PCBM BHJ solar cells with N-CNTs or B-CNTs. We note that this is the first success in the noticeable enhancement of organic-solar-cell performance by incorporating any one-dimensional nanomaterial, such as CNT, into the device active layer. Unlike undoped metallic multiwalled CNTs, which cause undesired electron–hole recombination, N- or B-CNTs uniformly dispersed in the active layer selectively enhance electron or hole transport, respectively, and eventually help carrier collection. In particular, the incorporation of 1.0 wt% B-CNTs results in balanced electron and hole transport, and accomplishes a power-conversion-efficiency improvement from 3.0% (conventional control cells without CNTs) to 4.1% (37% enhancement). The selective charge-transport enhancement in doped CNTs offers a general route to address the intrinsic low carrier mobility of organic-semiconductor-based optoelectronics and electric devices.[11,22,40,41]

Experimental Section

B- and N-Doping of CNTs: 95% purity multiwalled CNTs were purchased from Hanwha Nanotech. The CNTs were sonicated in a 1:3 v/v HNO_3/H_2SO_4 mixture for 10 h to remove metal catalysts, and subsequently thermally treated at 400 °C for 40 min to remove amorphous carbon species. The average diameter and length of the purified CNTs were 10–15 nm and <1 μm, respectively. For B-doping, 5:1 wt/wt B_2O_3/CNT powder mixture was thermally treated at 1100 °C for 4 h under Ar (40 sccm) and NH_3 (60 sccm) mixed gas flow. After thermal treatment, the remaining B_2O_3 powder was washed with hot boiled deionized (DI) water. For N-doping, the purified CNTs were thermally treated at 1100 °C for 4 h under Ar (40 sccm) and NH_3 (60 sccm) gas flow.

P3HT/PCBM/CNT Solution Preparation: The P3HT (Rieke metals, #4002-EE) and PCBM (Nano-C) mixture solution (1:0.7 wt) was prepared by dissolving in dichlorobenzene/chloroform(DCB/CF; 1:1 wt) cosolvent (concentration: 1.5 wt%) The undoped CNT, B-CNT, and N-CNT were supplementarily added into the solution, which was sonicated for 1 h. The CNT concentration was controlled to be 0.2, 1.0, 3.0, 5.0 wt% with respect to P3HT. The prepared solution was subsequently stirred for 24 h at 50 °C.

Organic Solar Cell Fabrication and Characterization: Solar cells were fabricated on ITO-coated glass substrates in a nitrogen-filled glove box. The substrates were cleaned in an ultrasonic bath with detergent, acetone, and 2-propanol and exposed to ultraviolet ozone (UVO) irradiation for 20 min. PEDOT:PSS was deposited by spin casting and dried for 30 min at 150 °C. The active layer, which consisted of P3HT/PCBM/CNT, was deposited by spin casting and dried for 10 min at 110 °C. The TiO_x solution was deposited by spin casting and oxidized under an atmospheric condition over 10 min. The fabricated photovoltaic cells were dried at 80 °C for 15 min in the glove box. The 100-nm Al electrode was deposited by thermal evaporation. After Al deposition, post-heat treatment was performed at 150 °C for 15 min. The active area surface was 4.0 mm^2. All the measurements were performed in a glove box, under illumination of simulated AM 1.5G irradiation (100 mW cm^{-2}) and using a xenon-lamp-based solar simulator (ABET LS-150-Xe).

Supporting Information

Supporting Information is available from the Wiley Online Library or from the author.

Acknowledgements

This work was supported by the National Research Laboratory Program (R0A-2008–000-20057–0), KAIST EEWS (EEWS: Energy, Environment, Water, and Sustainability) Initiative (EEWS0903), Center for Inorganic Photovoltaic Materials (ERC) (2008–0062204), and WCU (World Class University, R32–2008-000–10051-0) program funded by the Korean government. S. Yoo acknowledges the Korea Institute of Energy Technology Evaluation and Planning (KETEP) in Ministry of Knowledge Economy (MKE) under the New and Renewable Energy R&D Grant (N02090016).

Received: September 9, 2010
Revised: October 4, 2010
Published online: November 30, 2010

[1] G. Yu, J. Gao, J. C. Hummelen, F. Wudl, A. J. Heeger, *Science* **1995**, *270*, 1789.
[2] N. S. Sariciftci, L. Smilowitz, A. J. Heeger, F. Wudl, *Science* **1992**, *258*, 1474.
[3] F. Yang, M. Shtein, S. R. Forrest, *Nat. Mater.* **2005**, *4*, 37.
[4] G. Li, V. Shrotriya, J. Huang, Y. Yao, T. Moriarty, K. Emery, Y. Yang, *Nat. Mater.* **2005**, *4*, 864.
[5] S. H. Park, A. Roy, S. Beaupré, S. Cho, N. Coates, J. S. Moon, D. Moses, M. Leclerc, K. Lee, A. J. Heeger, *Nat. Photon.* **2009**, *3*, 297.
[6] W. U. Huynh, J. J. Dittmer, A. P. Alivisatos, *Science* **2002**, *295*, 2425.
[7] J. Liu, T. Tanaka, K. Sivula, A. P. Alivisatos, J. M. J. Fréchet, *J. Am. Chem. Soc.* **2004**, *126*, 6550.
[8] T. H. Han, W. J. Lee, D. H. Lee, J. E. Kim, E.-Y. Choi, S. O. Kim, *Adv. Mater.* **2010**, *22*, 2060.
[9] H. Ago, K. Petritsch, M. S. P. Shaffer, A. H. Windle, R. H. Friend, *Adv. Mater.* **1999**, *11*, 1281.
[10] S. Chaudhary, H. Lu, A. M. Müller, C. J. Bardeen, M. Ozkan, *Nano Lett.* **2007**, *7*, 1973.
[11] D. H. Lee, J. E. Kim, T. H. Han, J. W. Hwang, S. Jeon, S.-Y. Choi, S. H. Hong, W. J. Lee, R. S. Ruoff, S. O. Kim, *Adv. Mater.* **2010**, *22*, 1.
[12] A. J. Miller, R. A. Hatton, S. R. P. Silva, *Appl. Phys. Lett.* **2006**, *89*, 133117.
[13] A. J. Miller, R. A. Hatton, S. R. P. Silva, *Appl. Phys. Lett.* **2006**, *89*, 123115.
[14] R. H. Baughman, A. A. Zakhidov, W. A. de Heer, *Science* **2002**, *297*, 787.
[15] S. H. Lee, J. S. Park, B. K. Lim, C. B.Mo, W. J. Lee, J. M. Lee, S. H. Hong, S. O. Kim, *Soft Matter* **2009**, *5*, 2343.
[16] M. S. Dresselhaus, G. Dresselhaus, P. Avouris, *Carbon nanotubes: synthesis, structure, properties and applications*, Springer-Verlag: Berlin, Heidelberg, New York **2001**.
[17] S. Berson, R. de Bettignies, S. Bailly, S. Guillerez, B. Jousselme, *Adv. Funct. Mater.* **2007**, *17*, 3363.
[18] X. M. Liu, H. E. Romero, H. R. Gutierrez, P. C. Eklund, *Nano Lett.* **2008**, *8*, 2613.
[19] E. Borowiak-Palen, T. Pichler, A. Graff, R. J. Kalenczuk, M. Knupfer, J. Fink, *Carbon* **2004**, *42*, 1123.
[20] D. Golberg, Y. Bando, W. Han, K. Kurashima, T. Sato, *Chem. Phys. Lett.* **1999**, *308*, 337.
[21] J.-C. Charlier, M. Terrones, M. Baxendale, V. Meunier, T. Zacharia, N. L. Rupesinghe, W. K. Hsu, H. Terrones, G. A. J. Amaratunga, *Nano Lett.* **2002**, *2*, 1191.

[22] D. H. Lee, W. J. Lee, S. O. Kim, *Nano Lett.* **2009**, *9*, 1427.
[23] P. Ayala, J. Reppert, M. Grobosch, M. Knupfer, T. Pichler, A. M. Rao, *Appl. Phys. Lett.* **2010**, *96*, 183110.
[24] J. S. Park, B. R. Lee, J. M. Lee, J.-S Kim, S. O. Kim, M. H. Song, *Appl. Phys. Lett.* **2010**, *96*, 243306.
[25] T.-W. Koh, J. M. Choi, S. Lee, S. Yoo, *Adv. Mater.* **2010**, *22*, 1849.
[26] S. Braun, W. R. Salaneck, M. Fahlman, *Adv. Mater.* **2009**, *21*, 1450.
[27] Y. Park, V. Choong, Y. Gao, B. R. Hsieh, C. W. Tang, *Appl. Phys. Lett.* **1996**, *68*, 2699.
[28] V. D. Mihailetchi, H. Xie, B. de Boer, L. J. A. Koster, P. W. M. Blom, *Adv. Funct. Mater.* **2006**, *16*, 699.
[29] G. Li, C.-W. Chu, V. Shrotriya, J. Huang, Y. Yang, *Appl. Phys. Lett.* **2006**, *88*, 253503.
[30] S. Han, S. Lim, H. Kim, H. Cho, S. Yoo, *IEEE J. Sel. Top. Quantum Electron.* **2010**, DOI: 10.1109/JSTQE.2010.2041637.
[31] V. D. Mihailetchi, J. K. J. van Duren, P. W. M. Blom, J. C. Hummelen, R. A. J. Janssen, J. M. Kroon, M. T. Rispens, W. J. H. Verhees, M. M. Wienk, *Adv. Funct. Mater.* **2003**, *13*, 43.
[32] S. Scheinert, W. Schliefke, *Synt. Met.* **2003**, *139*, 501.
[33] M. M. Mandoc, L. J. A. Koster, P. W. M. Blom, *Appl. Phys. Lett.* **2007**, *90*, 133504.
[34] K. Lee, J. Y. Kim, S. H. Park, S. H. Kim, S. Cho, A. J. Heeger, *Adv. Mater.* **2007**, *19*, 2445.
[35] J. Y. Kim, K. Lee, N. E. Coates, D. Moses, T.-Q. Nguyen, M. Dante, A. J. Heeger, *Science* **2007**, *317*, 222.
[36] S. D. Bergin, V. Nicolosi, P. V. Streich, S. Giordani, Z. Sun, A. H. Windle, P. Ryan, N. P. P. Niraj, Z.-T. T. Wang, L. Carpenter, W. J. Blau, J. J. Boland, J. P. Hamilton, J. N. Coleman, *Adv. Mater.* **2008**, *20*, 1.
[37] S. H. Lee, J. S. Park, C. M. Koo, B. K. Lim, S. O. Kim, *Macromol. Res.* **2008**, *16*, 261.
[38] B. K. Lim, S. H. Lee, J. S. Park, S. O. Kim, *Macromol. Res.* **2009**, *17*, 666.
[39] S. H. Lee, J. S. Park, B. K. Lim, S. O. Kim, *J. Appl. Polym. Sci.* **2008**, *110*, 345.
[40] D. H. Lee, W. J. Lee, S. O. Kim, *Chem. Mater.* **2009**, *21*, 1368.
[41] D. H. Lee, D. O. Shin, W. J. Lee, S. O. Kim, *Adv. Mater.* **2008**, *20*, 2480.